Tellus (1989), *41A*, 275–284

On the structure of potential vorticity in baroclinic instability

By WALTER A. ROBINSON, *Department of Atmospheric Sciences, University of Illinois, Urbana, IL 61801, USA*

(Manuscript received 20 June 1988; in final form 13 September 1988)

ABSTRACT

The structure of baroclinic modes is examined in terms of their potential vorticity. Baroclinic instabilities may be viewed as mutually reinforcing interactions between the disturbance potential vorticity at different levels in the atmosphere. A technique is introduced for diagnosing quantitatively which levels of potential vorticity are important in the growth of the instability. Both Charney and Green modes are found to depend on the interaction between the surface thermal anomalies and a thin layer of potential vorticity anomalies centered on the steering level. In the Green modes, the growth is retarded by the influence of the eddy potential vorticity at higher levels. The inclusion of a tropopause in the basic state does not modify the fundamental dynamics of the baroclinic modes in the presence of linear shear.

1. Introduction

Baroclinic instability, the growth of initially weak disturbances on a vertically sheared basic state, is fundamental to our modern understanding of the dynamics of the extra-tropical atmosphere. Because it is basic to how meteorologists look at the atmosphere, it is desirable to understand fully how baroclinic instability works. One approach towards better understanding baroclinic instability, taken by Lindzen and his collaborators, has been to treat the instability as a particular case of wave over-reflection (Lindzen and Tung, 1978; Lindzen et al., 1980). Another approach is to consider the structure of baroclinic waves in terms of their potential vorticity. This view of baroclinic instability was introduced by Bretherton (1966a, b), and was reviewed by Hoskins et al. (1985). While these two approaches are not mutually exclusive, they focus on different ways in which regions of the atmosphere communicate. The over-reflection approach emphasizes communication by the propagation of Rossby wave activity on a time scale determined by the group velocity of the waves and the distance over which they must travel. The potential vorticity approach stresses communication on the time scale in which the flow achieves geostrophic balance. In the quasi-geostrophic system this is assumed to occur immediately. The present work quantitatively extends the potential vorticity approach to baroclinic instability.

The utility of the potential vorticity perspective depends on two properties of the potential vorticity (Hoskins et al., 1985): its conservation following fluid motion in frictionless adiabatic flow and its invertibility. Invertibility is shorthand for the fact that given the potential vorticity, appropriate boundary conditions, and a condition of balance for the flow, the flow (winds, pressures, and temperatures) is uniquely determined and can be obtained by the inversion of an elliptic operator. The two properties together lead to a conceptually simple depiction of atmospheric dynamics wherein the flow rearranges potential vorticity; the new distribution of potential vorticity determines a new flow that further rearranges the potential vorticity, and so on.

Because the operator that takes the streamfunction into the potential vorticity resembles the Laplacian, qualitative inversion of potential vorticity distributions is straightforward. Flow is cyclonic about positive potential vorticity anomalies, and anticyclonic about negative anomalies. The flow induced by an anomaly decays away from the anomaly, and larger scale features in the potential vorticity are more effective in inducing winds than are smaller scale features. In short, the streamfunction is a smoothed version of the potential vorticity, with a change of sign.

An important addition to the potential vorticity approach, contributed by Bretherton (1966a), was the realization that thermal structure at a horizontal boundary behaves identically to a thin sheet of intense structure in the potential vorticity immediately above or below the boundary, Warm regions at the ground induce cyclonic flow aloft, while cool regions induce anticyclonic flow.

The potential vorticity view of baroclinic instability was introduced by Bretherton (1966b) in order to explain the short wave cut-off for baroclinic instability in the two-layer and Eady (1949) models. Consider two atmospheric layers, both containing a zonal flow and a wavelike perturbation. The zonal westerly flow, $\bar{u}$ is greater in the upper than in the lower layer, and the gradient of the potential vorticity of the mean flow, $\bar{q}_y$, is positive in the upper layer and negative in the lower layer. The potential vorticity anomalies in each layer induce meridional flow in the other layer, southerly flow to the west of negative anomalies and northerly flow to the west of positive anomalies. If the pattern of anomalies in the upper layer is shifted to the west relative to that in the lower layer then the northerly flow induced by the positive anomalies in the lower layer will advect mean flow potential vorticity down its gradient into the positive anomalies in the upper layer, reinforcing the upper layer anomalies. Similarly the southerly flow induced by the positive anomalies in the upper layer will carry potential vorticity down its gradient into the positive anomalies in the lower layer reinforcing the lower layer anomalies.

The flows induced in the other layer by each layer of anomalies must be strong enough to keep the disturbance from being pulled apart by the shear of the zonal flow. The strength of the induced flow decreases as the wavenumber of the disturbance increases, and as the separation between the layers increases.

In the Charney (1947) model, the lower layer is at the ground but the position of the upper layer is unconstrained. As the wavenumber of the disturbance is increased, the depth of the flow induced by the surface thermal anomalies decreases and the structure of the instability is squeezed closer to the lower boundary. In the Eady model, the upper layer is the upper boundary of the domain, so the separation between the layers is fixed. As the wavenumber of the disturbance increases the strength of the flow induced by each layer in the other decreases. Eventually they are unable to keep each other "in step" against the shear of the zonal flow, and the instability is lost. This is the essence of Bretherton's (1966b) explanation of the short wave cut-off, and it applies equally well to the two-layer model and to Read's (1988) finding that the wavelength of greatest instability increases in a compressible Eady model with the depth of the domain.

The purpose of the present study is to locate the dynamically important potential vorticity in baroclinic modes, and thereby make quantitative the conceptual model of baroclinic instability described above. The method employed is to calculate how potential vorticity at some level contributes to the zonally averaged meridional flux of potential vorticity at other levels. Section 2 describes the theoretical basis for the calculations. Results for the Charney (1947) and Green (1960) modes are presented in Section 3. Section 4 describes calculations for basic states that include a tropopause and discusses the relevance of Eady dynamics to the atmosphere. A summary of the results is in the final section.

2. Theory

Consider disturbances whose evolution obeys the quasi-geostrophic potential vorticity equation, linearized about a zonally symmetric basic state:

$$q_t + \bar{u} q_x + v \bar{q}_y = 0, \tag{1}$$

where the overbars indicate zonal averages and their absence denotes eddy quantities; u is the zonal wind, v is the meridional wind, and q is the quasi-geostrophic eddy potential vorticity, given by,

$$q = \nabla^2 \psi + \rho^{-1} \partial/\partial z(\rho \varepsilon \psi_z), \tag{2}$$

where ψ is the eddy geostrophic streamfunction; ρ is a basic state density given by $\rho = \rho_0 \exp(-z/H)$; ε is a stability parameter given by $\varepsilon = f_0^2/N^2$ where f_0 is the coriolis parameter in the center of the domain and N is the buoyancy frequency; z is a log-pressure vertical coordinate $z = H \ln(p_0/p)$. The meridional derivative of the mean flow potential vorticity, $\bar{q}_y$, is given by

$$\bar{q}_y = \beta - \rho^{-1}\, \partial/\partial z(\rho \varepsilon \bar{u}_z), \tag{3}$$

where β is the meridional derivative of the coriolis parameter, i.e., $f(y) = f_0 + \beta y$. The appropriate boundary conditions on (1) are that the density of disturbance energy be bounded for large z, and that at $z = 0$,

$$\psi_{zt} + \bar{u}\psi_{zx} - v\bar{u}_z = 0. \tag{4}$$

The meridional wind is assumed to vanish on the vertical boundaries, at $y = \pm L/2$.

An equation for the perturbation energy per unit area is obtained from multiplying (1) by the perturbation streamfunction, ψ, and integrating over the mass of the domain,

$$E_t = -(1/L)\int_0^{\infty}\int_{-L/2}^{L/2} \mathrm{d}y\, \mathrm{d}z\, \bar{u}F, \tag{5}$$

where the energy, E, is given by,

$$E = (1/L)\int_0^{\infty}\int_{-L/2}^{L/2} \mathrm{d}y\, \mathrm{d}z\, \rho/2[u^2 + v^2 + \varepsilon\psi_z^2]. \tag{6}$$

F is the mass weighted zonally averaged northward flux of potential vorticity,

$$F = \rho\overline{vq} + \delta(z)\rho\overline{v\psi_z}, \tag{7}$$

where δ is the delta function. Similarly, the evolution of the perturbation potential enstrophy, Q, per unit area at any level is obtained by multiplying (1) by the eddy potential vorticity and integrating,

$$Q_t(z) = -(1/L)\int_{-L/2}^{L/2} \mathrm{d}y\, \bar{q}_y F/\rho, \tag{8}$$

where Q is given by,

$$Q = (1/L)\int_{-L/2}^{L/2} \mathrm{d}y\, \overline{q^2}/2. \tag{9}$$

In an unstable baroclinic mode the energy and the potential enstrophy show the same exponential increase with time. As indicated by (5) and (9), the growth of both quantities depends on the structure of the northward flux of potential vorticity, F. Bretherton (1966a) showed that the domain integral of F vanishes. Thus from (5) and (9) it is seen that for a growing wave F must be negatively correlated with $\bar{q}_y$ and with $\bar{u}$. Lindzen et al. (1980) discuss the vertical distributions of F for solutions to the Charney problem.

The approach in the present study is to diagnose the interactions between potential vorticity at different levels that contribute to F. Consider a disturbance with the horizontal structure,

$$\psi(x, y, z) = \mathrm{Real}[\Psi(z)\, \mathrm{e}^{ikx}]\sin(ly). \tag{10}$$

The meridional flux of potential vorticity at a given level, z, can be constructed from the contributions to that flux from the meridional velocities at z induced by potential vorticity at other levels. Let $G_k(z, z')$ be the Green function for the potential vorticity operator for the wave,

$$\partial/\partial z[\rho(z)\varepsilon\, \partial G_k(z, z')/\partial z] - \rho(z)K^2 G_k(z, z') = \rho(z)\delta(z - z'), \tag{11}$$

where $K^2 = k^2 + l^2$. Then the contribution to the flux at z induced by potential vorticity at z' is given by,

$$\Delta F(z, z') = \rho(z)G_k(z, z')\overline{q(z)q_x(z')}, \tag{12}$$

where

$$F(z) = \int_0^{\infty} \mathrm{d}z'\, \Delta F(z, z').$$

The differential operator in (11) is self-adjoint, so that,

$$\rho(z)G_k(z, z') = \rho(z')G_k(z', z). \tag{13}$$

Using the identity, $\overline{a_x b} = -\overline{a b_x}$, then yields the principal result,

$$\Delta F(z, z') = -\Delta F(z', z). \tag{14}$$

The northward flux of potential vorticity induced at some level by potential vorticity at some other level is equal and opposite to the flux at the latter level induced by the potential vorticity at the former level. More generally, this result holds for the interaction between different latitudes as well as different altitudes, and there is no requirement that the disturbance be wavelike or that its amplitude be small.

Baroclinic instability can be understood as comprising the interactions between many pairs of levels, z and z'. Such interactions contribute to F with opposite signs at the two levels, and so can reinforce the disturbance at both levels only if the sign of $\bar{q}_y$ changes between them. In classic baroclinic instability problems, such as the Charney problem, the mutually reinforcing interactions are those between the surface and the interior of the atmosphere.

The remainder of this paper presents calculations of ΔF for various linear baroclinic modes. From the potential vorticity perspective, such calculations reveal which regions are dynamically important in the growth of baroclinic instabilities. The baroclinic modes are computed by a simple numerical integration in time of (1) on a vertical grid with a resolution of 20 points per scale height. The integration is continued until a constant growth rate and phase speed are achieved. The model has a lid at five scale heights where the perturbation streamfunction is forced to vanish; the structure of the modes in the lower atmosphere proved insensitive to the height of the lid when it is at least this high. Calculations are performed for an infinitely wide channel; i.e., $l = 0$.

Eq. (1) is non-dimensionalized with the following scaling: height is scaled by H; horizontal lengths are scaled by the Rossby radius of deformation, $L_D = H/\sqrt{\varepsilon}$; and time is scaled by $\tau = (L_D \beta)^{-1}$. Thus, for typical middle-latitude conditions, $L_D = 10^3$ km; $\beta = 1.5 \times 10^{-11}$ (m s)$^{-1}$, a single unit of non-dimensional time corresponds to approximately 0.75 days, and unit non-dimensional horizontal velocity corresponds to 15 m s^{-1}. The non-dimensional forms of (2) and (3) are,

$$q = \nabla^2 \psi + \psi_{zz} - \psi_z, \tag{15}$$

$$\bar{q}_y = 1 - \bar{u}_{zz} + \bar{u}_z. \tag{16}$$

3. Results for constant static stability

We consider first a Charney mode with non-dimensional wavenumber, $k = 2$, in a basic state with unit shear, $\bar{u} = z$ (dimensionally, this is a shear of approximately 2 m (s km)$^{-1}$). This mode has a growth rate of 0.29 and a phase speed of 0.30. Figs. 1 and 2 show the structure of the streamfunction and potential vorticity, amplitude and phase, in the lowest two scale heights of the atmosphere. The curves in Fig. 1 are familiar: strong trapping of the disturbance near the lower boundary and the rapid westward slope through the steering level giving way to nearly equivalent barotropic structure aloft. Fig. 2 is perhaps less familiar, particularly in that it shows the potential vorticity sloping to the east with height. Hoskins and Heckley (1981) showed that a similar eastward slope is present in the thermal structure of baroclinic waves.

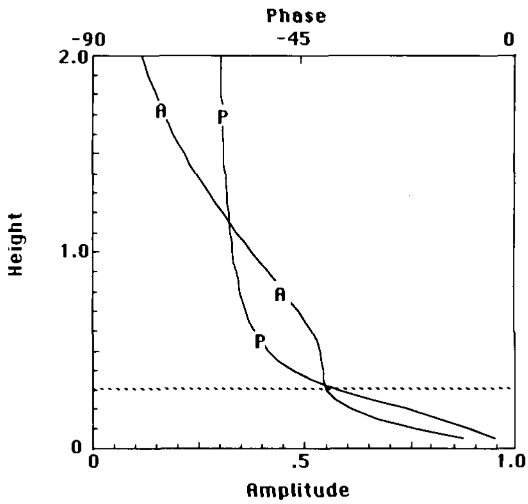

Fig. 1. Amplitude, curve "A", and phase (in degrees), curve "P", of the streamfunction for the $k = 2$ Charney mode in a mean flow with $\bar{u} = z$. The dashed line indicates the steering level.

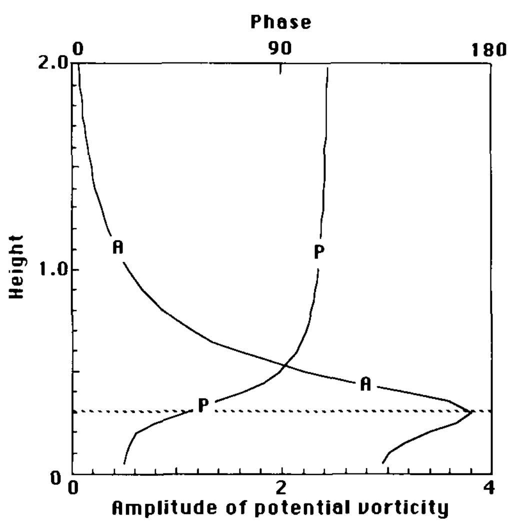

Fig. 2. As in Fig. 1, but for the potential vorticity.

The mass weighted northward flux of potential vorticity in this baroclinic wave is shown in Fig. 3, the curve labeled "T". The flux is everywhere southward, with strongest values at, and decaying rapidly with height above, the steering level, structure noted for a similar Charney mode by Lindzen et al. (1980).

The curve labeled "S" shows $\Delta F(z, 0)$, the flux of potential vorticity in the free atmosphere induced by the surface thermal anomalies. With a change of sign this curve also indicates how potential vorticity at each level in the atmosphere contributes to the northward flux of heat at the surface. Thus curve "S" shows the strength of the mutually reinforcing interaction of each level of potential vorticity with the temperature at the surface. The instability is maintained by the interaction of the temperature at the surface with a thin layer of potential vorticity centered immediately above the steering level. A layer of potential vorticity distributed through the atmosphere according to curve S can be identified with the upper layer in Hoskin et al.'s (1985) qualitative schematic of baroclinic instability. The importance of the region surrounding the steering level is also consistent with the theory of overreflection (Lindzen et al., 1980).

From Fig. 3 it is seen that the interaction between the surface and the atmosphere below the steering level is weak (curve "S") and cannot explain the strong southward flux of potential vorticity in this region. Potential vorticity at these levels is driven southward by the flow induced by potential vorticity in overlying layers. This is seen from Fig. 4, which shows $\Delta F(z, 3.5)$, the contribution to the flux of potential vorticity elsewhere from the potential vorticity at $z = 3.5$, the maximum of curve "S" in Fig. 3. Consistent with the eastward slope with height of the potential vorticity, potential vorticity near $z = 3.5$ induces a southward flux of potential vorticity at lower levels. The disturbance at and above the steering level grows by its interaction with the surface. From these levels the disturbance is communicated downward to fill the region between the steering level and the ground.

The structure of a Green (1960) mode is very different. Figs. 5, 6 show the amplitude and phase of the disturbance streamfunction and potential vorticity for a mode with $k = 0.6$ on the same basic state as before. This wave has a phase speed of 0.35 and a growth rate of 0.05. Both the streamfunction and the potential vorticity have local minima at $z = 0.55$. The streamfunction slopes to the west with height throughout the lower atmosphere, while the phase of the potential vorticity slopes to the east below $z = 0.45$ and to the west above.

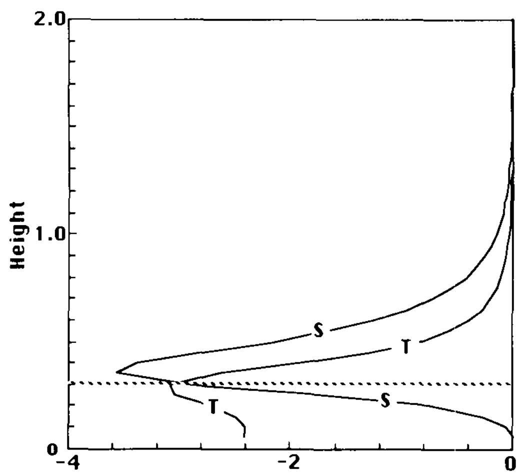

Fig. 3. The mass weighted meridional flux of potential vorticity, F, for the $k = 2$ Charney mode. Curve "T" shows the total flux and curve "S" shows that induced by the surface. The dashed line indicates the steering level.

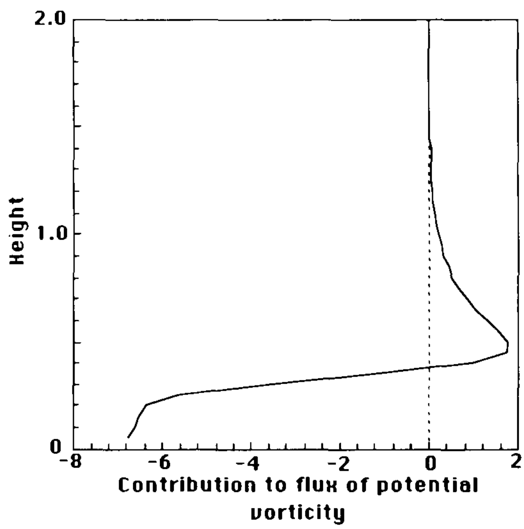

Fig. 4. $\Delta F(z, 3.5)$, the contribution of potential vorticity at $z = 3.5$ to $F(z)$, for the $k = 2$ Charney mode.

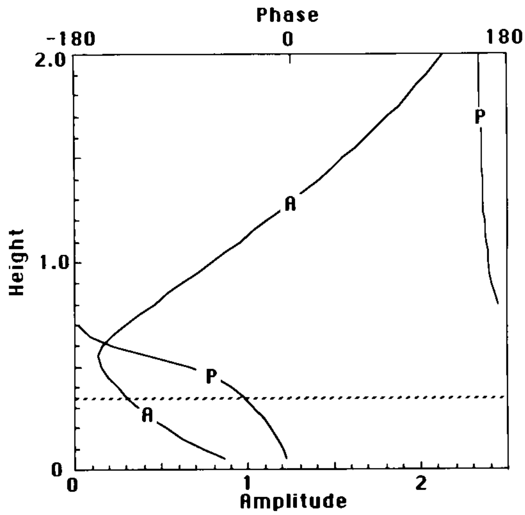

Fig. 5. As in Fig. 1, but for the $k = 0.6$ Green mode.

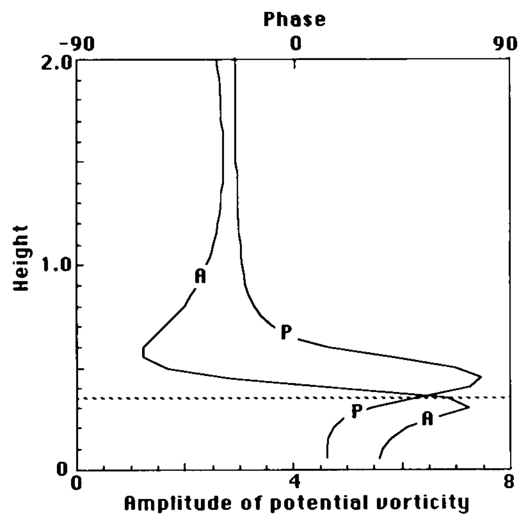

Fig. 6. As in Fig. 2, but for the $k = 0.6$ Green mode.

The flux of potential vorticity, the total and that induced by the surface, are shown in Fig. 7. Several features of these curves are noteworthy. First, unlike the Charney mode, the total flux is much smaller in magnitude than that induced by the interaction with the surface. This implies the existence of interactions among atmospheric levels that nearly cancel the interactions with the surface. For example, potential vorticity at the steering level induces a southward flux of potential vorticity at levels around $z = 1.0$ that opposes the northward flux induced from the surface (Fig. 8). The net flux must be everywhere southward if the disturbance is to grow (Eq. 8).

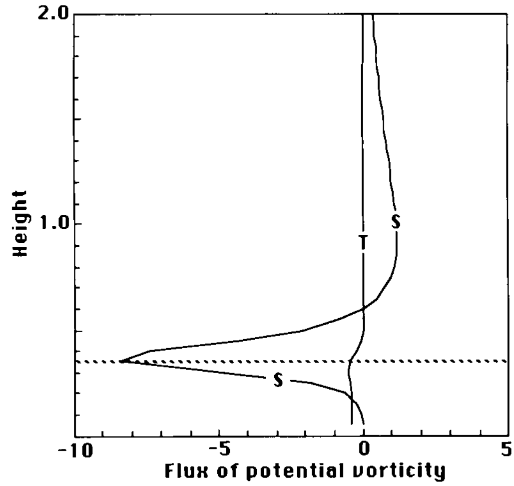

Fig. 7. As in Fig. 3, but for the $k = 0.6$ Green mode.

Using relation (14) it is seen from Figs. 7 and 8 that the upper lobe of the disturbance potential vorticity induces fluxes at the surface and at the steering level that oppose the growth of the instability, i.e., the upper lobe induces a southward flux of heat at the surface and a northward

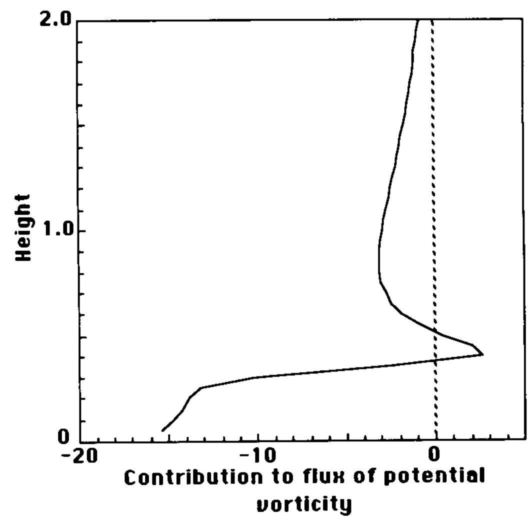

Fig. 8. $\Delta F(z, 3.5)$ for the $k = 0.6$ Green mode.

flux of potential vorticity at the steering level. From the potential vorticity perspective the upper lobe of the Green mode is parasitic on the mutually reinforcing interaction between the surface and the steering level that drives the instability. This is in contrast with the traditional view that would focus on the energy releasing northward flux of heat in the upper lobe.

The strong direct interaction between the upper troposphere and the surface is possible in this wave, because its low wavenumber permits the flow induced by the potential vorticity to extend over more than a scale height. The importance of this upper lobe in opposing the growth of the instability may be seen quantitatively in Fig. 9 (the curve labeled ".6"), which shows the vertically integrated fractional contribution of the potential vorticity in the atmosphere to the flux of heat at the surface, i.e., $\int_0^{z'} \mathrm{d}z' \Delta F(0,z')/F(0)$. Bearing in mind that this curve has a value of unity at the top of the domain ($z = 5.0$), it is seen that the growth-opposing interaction with the upper lobe cancels almost $\frac{7}{8}$ of the northward flux of heat induced by the interaction with potential vorticity below $z = 0.6$.

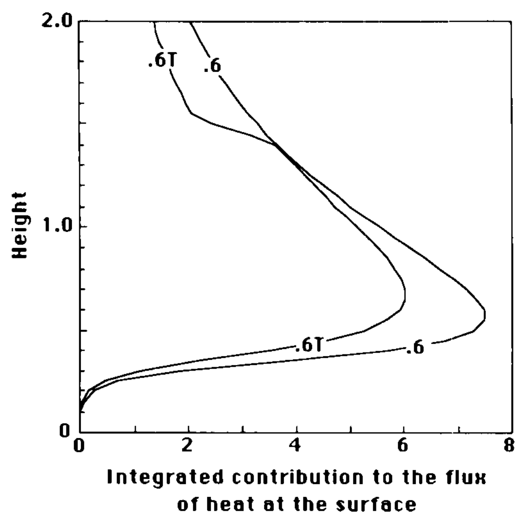

Fig. 9. Vertically integrated fractional contribution of the potential vorticity at z to the northward flux of heat at the surface, $\Delta F(0,z)$, for the $k = 0.6$ Green mode, curve ".6", and the 0.6 Green mode in the presence of a tropopause at $z = 1.5$, curve ".6T".

4. The effect of the tropopause

For present purposes the tropopause is defined as a jump in the static stability going from the troposphere to the stratosphere. This jump adds a contribution to $\bar{q}_y$ given by,

$$-\Delta\varepsilon\, U_z \delta(z - z_{\mathrm{T}}), \tag{17}$$

where $\Delta\varepsilon$ is the difference between the stratospheric and tropospheric values of ε, δ is the delta function, and z_{T} is the height of the tropopause. Because the static stability is greater in the stratosphere, $\Delta\varepsilon$ is negative. For westerly shear expression (17) leads to a sheet of potential vorticity at the tropopause increasing northward. In the Eady model the rigid lid implies an infinite static stability in the stratosphere, or $\Delta\varepsilon = -\varepsilon$. In fact, in the Eady model the only positive gradient of the potential vorticity of the mean flow is at the lid, and the disturbance grows by the mutually reinforcing interaction between the thermal anomalies at the lid, and those at the surface, there being no potential vorticity in the interior.

In examining the structure of baroclinic modes in the presence of a tropopause, Eady dynamics can be said to operate if the interaction of the surface with the tropopause dominates the interaction of the surface with the rest of the troposphere. In the cases described below the tropopause is placed at $z = 1.5$, corresponding to 223 mb. The buoyancy frequency in the stratosphere is taken to be twice that in the troposphere, so that ε(stratosphere) $= 0.25\varepsilon$(troposphere).

Clearly, potential vorticity at the tropopause can be important only if the wave has a significant amplitude at that level. The $k = 2$ Charney mode described in the previous section is essentially unchanged in the presence of a tropopause. While the amplitude and phase of the $k = 0.6$ Green mode is only altered slightly, the tropopause brings about a significant change in the structure of its potential vorticity. Fig. 10 shows that the surface induces a strong northward flux of potential vorticity at the tropopause for this Green mode. The flux at the tropopause opposes the instability, the opposite role to that played by the upper lid in the Eady model. The integral contribution of the tropopause to the surface flux of heat is modest, as may be seen from curve "0.6T" in Fig. 9. The tropopause accounts for

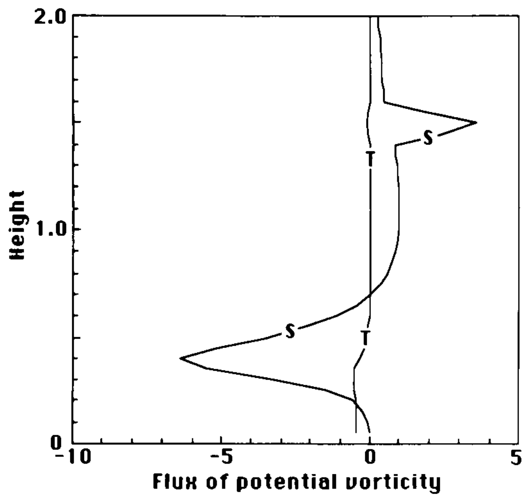

Fig. 10. As in Fig. 3, but for the $k = 0.6$ Green mode with a tropopause.

approximately 40% of the negative contribution to the flux of heat at the surface from the upper lobe of potential vorticity.

Charney modes can also extend higher into the atmosphere, if the vertical shear of the basic state is increased (Held, 1978). In the present scaling the relevant parameter, r (Pedlosky, 1979) is given by,

$$r = (1/\lambda + 1)(4k^2 + 1)^{1/2}, \tag{18}$$

where the mean flow is given by $U = \lambda z$. The fastest growing modes have values of r close to $\frac{1}{2}$ (Pedlosky, 1979). If we set $r = \frac{1}{2}$, then k is given by,

$$k = \tfrac{1}{2}[4(1 + 1/\lambda)^2 - 1]^{1/2}. \tag{19}$$

The wavenumber of the fastest growing mode decreases from ∞ to 0.866 as the vertical shear, λ, is increased from 0 to ∞. From the potential vorticity perspective the depth of the fastest growing mode increases with decreasing wavenumber, and thus with increasing shear, because the depth of the flows induced by the perturbation potential vorticity and perturbation surface temperature increase with the increasing horizontal scale of the disturbance.

The largest value of λ that compares reasonably with the earth's atmosphere is $\lambda = 5.0$. For this value the fastest growing wave has a horizontal wavenumber close to 1. Fig. 11 (the curve labeled "1") shows the amplitude of the $k = 1$ mode when $\bar{u} = 5z$ and Fig. 12 shows the amplitude and phase of its potential vorticity. The phase speed is 3.07 and the growth rate is 1.53. Figs. 11 and 12 show that the mode extends much further into the atmosphere than the severely trapped $k = 2$ mode discussed above. This is confirmed by Fig. 13 (curves "1" and "2") which

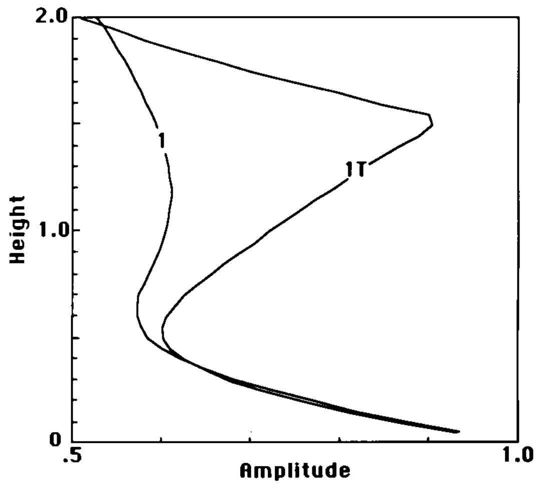

Fig. 11. The amplitude of the streamfunction of the $k = 1$ Charney mode with $\bar{u} = 5z$, in the absence, curve "1", and presence, curve "1T", of a tropopause at $z = 1.5$.

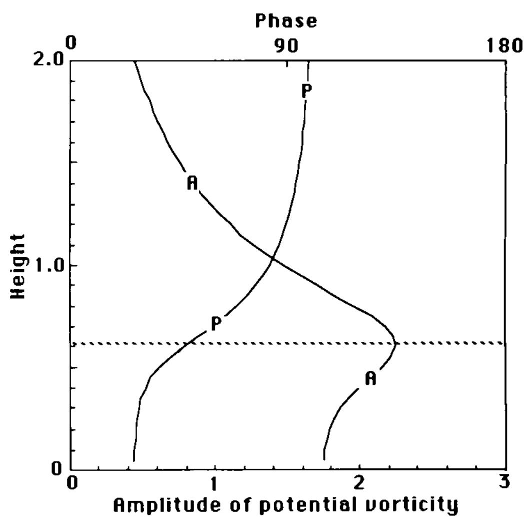

Fig. 12. As in Fig. 2 but for the $k = 1$ Charney mode with no tropopause.

shows that while for $k = 2$, most of the interaction with the surface comes from potential vorticity below $z = 0.5$, for $k = 1$ there is a substantial contribution from potential vorticity above $z = 1$.

When a tropopause is added to the mean flow, the vertical structure of this mode changes substantially. Its amplitude (Fig. 11, curve "1T") has a strong local maximum at the tropopause. In fact, within the troposphere the structure is reminiscent of the unstable Eady wave. From Fig. 14 it is seen that there is a strong interaction between the surface and the tropopause; in this case this interaction contributes to the growth of the instability. Returning to Fig. 13, however, we see that once again the integrated contribution of the tropopause to the heat flux at the surface is modest, less than 30% of the total. Even in this case of a very deep Charney mode, Eady dynamics are relatively unimportant in the growth of the wave.

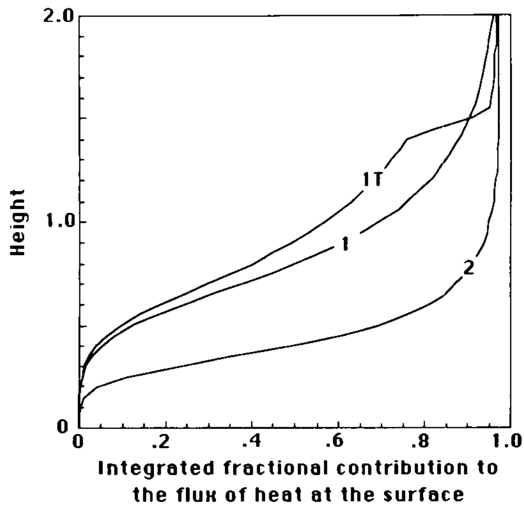

Fig. 13. As in Fig. 9, but for the $k = 2$ Charney mode with $\bar{u} = z$, curve "2", the $k = 1$ Charney mode with $\bar{u} = 5z$, curve "1", and the $k = 1$ Charney mode in the presence of a tropopause, curve "1T".

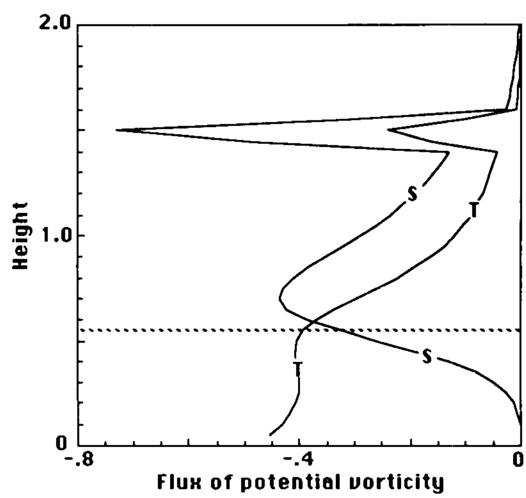

Fig. 14. As in Fig. 3, but for the $k = 1$ Charney mode with a tropopause.

5. Summary and conclusions

A quantitative approach to diagnosing the interactions between potential vorticity at different levels has been introduced. The results for Charney mode baroclinic waves confirms the schematic of Hoskins et al., and provides an identification of the lower level of potential vorticity with the thermal structure at the surface, and the upper level with a thin region of potential vorticity at and above the steering level. In the case of a Green mode, the disturbance is maintained by the same mutually reinforcing interaction between surface temperature and potential vorticity at the steering level, but in this case the growth rate is severely reduced by the parasitic nature of the upper lobe of the disturbance.

The tropopause is shown to introduce a thin sheet of northward increasing potential vorticity in mean flows with positive vertical shear. In the Eady model, waves are sustained entirely by the interaction between the surface temperature and the potential vorticity at the tropopause (the temperature at the lid). The applicability of the Eady model to an unbounded compressible atmosphere depends on the interactions between the tropopause and the surface being more important than interactions between the surface and potential vorticity in the troposphere. In linear baroclinic modes growing in the presence of constant vertical shear and a tropopause Eady dynamics, in this sense, are found to be relatively unimportant.

6. Acknowledgements

This work was begun at the Department of Atmospheric Sciences at the University of Washington under the support of NASA grant NAGW-662, and was completed at the Department of Atmospheric Sciences at the University of Illinois at Urbana-Champaign through the generous support of the Department.

REFERENCES

Bretherton, F. P. 1966a. Critical layer instability in baroclinic flows. *Quart. J. R. Met. Soc. 92*, 325–334.

Bretherton, F. P. 1966b. Baroclinic instability and the short wavelength cut-off in terms of potential vorticity. *Quart. J. R. Met. Soc. 92*, 335–345.

Charney, J. G. 1947. The dynamics of long waves in a baroclinic westerly current. *J. Met. 4*, 135–162.

Eady, E. T. 1949. Long waves and cyclone waves. *Tellus 1, no. 3*, 33–52.

Green, J. S. A. 1960. A problem in baroclinic instability. *Quart. J. R. Met. Soc. 86*, 237-251.

Held, I. M. 1978. The vertical scale of an unstable baroclinic wave and its importance for eddy heat flux parameterizations. *J. Atmos. Sci. 35*, 572–576.

Hoskins, B. J. and Heckley, W. A. 1981. Cold and warm fronts in baroclinic waves. *Quart. J. R. Met. Soc. 107*, 79–90.

Hoskins, B. J., McIntyre, M. E. and Robertson, A. W. 1985. On the use and significance of isentropic potential vorticity maps. *Quart. J. R. Met. Soc. 111*, 877–946.

Lindzen, R. S. and Tung, K.-K. 1978. Wave over-reflection and shear instability. *J. Atmos. Sci. 35*, 1626–1632.

Lindzen, R. S., Farrell, B. and Tung, K.-K. 1980. The concept of wave over-reflection and its application to baroclinic instability. *J. Atmos. Sci. 37*, 44–63.

Pedlosky, J. 1979. *Geophysical fluid dynamics.* New York: Springer-Verlag, 624 pp.

Read, P. L. 1988. On the scale of baroclinic instability in deep, compressible atmospheres. *Quart. J. R. Met. Soc. 114*, 421–437.